T-odd correlation in the $K_{l3\gamma}$ decay

V. V. Braguta
Moscow Institute of Physics and Technology, Dolgoprudny 141700, Russia

A. A. Likhoded*
Institute for High Energy Physics, Protvino, 142284 Russia

A. E. Chalov
Moscow Institute of Physics and Technology, Dolgoprudny 141700, Russia

(Received 12 October 2001; published 20 February 2002)

The dependence of the $K^+\to\pi^0 l^+\nu_l\gamma$ decay width on the T-odd kinematical variable $\xi=\vec{q}\cdot[\vec{p}_l\times\vec{p}_\pi]/M^3$ is studied at the tree and one-loop levels of the standard model (SM). It is shown that at the tree level this decay width is an even function of ξ, while the odd contribution arises due to the electromagnetic final state interaction. This contribution is determined by the imaginary parts of the one-loop diagrams. The calculations performed show that the ξ-odd contribution to the $K^+\to\pi^0 e^+\nu_e\gamma$ and $K^+\to\pi^0\mu^+\nu_\mu\gamma$ decay widths is four orders of magnitude smaller than the even contribution coming from the tree level of the SM.

DOI: 10.1103/PhysRevD.65.054038 PACS number(s): 13.20.Eb, 11.30.Er

I. INTRODUCTION

The study of rare radiative K-meson decays provides an interesting possibility to search for the effects of a new physics beyond the standard model (SM). In particular, the search for new CP-violating interactions is of special interest. In contrast to the SM, where CP violation is caused by the presence of the complex phase in the Cabibbo-Kabayashi-Maskawa (CKM) matrix, CP violation in extended models can naturally arise due to the presence of, for instance, new charged Higgs bosons, which have complex couplings to fermions [1], hypothetical tensor interactions [2], etc. CP-violating effects can be probed with experimental observables, which are especially sensitive to T-odd contributions. Such observables are the rate dependence on the T-odd correlation ($\xi=(1/M_K^3)\vec{p}_\gamma\cdot[\vec{p}_\pi\times\vec{p}_l]$) in the $K^\pm\to\pi^0\mu^\pm\nu\gamma$ process [3] and transverse muon polarization in the $K^\pm\to\mu^\pm\nu\gamma$ decays [4]. The experiments conducted thus far do not provide the sensitivity level that is necessary to analyze the differential distributions in the $K^\pm\to\pi^0\mu^\pm(e^\pm)\nu\gamma$ decays. However, new perspectives are connected with the planned OKA experiment [5], where the expected statistics of $\sim 7.0\times 10^5$ events for the $K^+\to\pi^0\mu^+\nu\gamma$ decay will allow one to perform a detailed analysis of the data and either probe new effects or put strict bounds on the parameters of the extended models.

When searching for possible T-violating effects caused by new interactions in the $K^+\to\pi^0\mu^+\nu\gamma$ decays it is especially important to estimate the SM contribution to the ξ distribution, which is induced by the electromagnetic final state interaction and which is a natural background for new interaction contributions.

The Weinberg model with three Higgs doublets [1,6] is especially interesting in the search for possible T violation. This model allows one to have complex Yukawa couplings that lead to extremely interesting phenomenology. It was shown [3] that the study of the T-odd correlation in the $K^+\to\pi^0\mu^+\nu\gamma$ process allows one either to probe the terms that are linear in CP-violating couplings, or to strictly confine the Weinberg model parameters.

In this paper, in the framework of the SM we analyze the $K^+\to\pi^0 l^+\nu_l\gamma$ decay width dependence on the kinematical variable $\xi=\vec{q}\cdot[\vec{p}_l\times\vec{p}_\pi]/M^3$. In the general case, the width differential distribution $\rho(\xi)=d\Gamma/d\xi$ can be represented as the sum of even, f_{even}, and odd, f_{odd}, functions of ξ. At the tree level of the SM the odd part f_{odd} does not contribute to the width distribution. We will show later that this effect is a direct consequence of the following fact: in chiral perturbation theory the form factors contributing to the matrix element do not have imaginary parts. However, the SM radiative corrections due to the electromagnetic final state interaction lead to the appearance of form factor imaginary parts [7], which, in its turn, results in a nonvanishing ξ-odd contribution in the $K^+\to\pi^0 l^+\nu_l\gamma$ decay width distribution. In this paper we analyze this effect at the one-loop level of the SM. The matrix element of the $K^+\to\pi^0 l^+\nu_l\gamma$ decay is calculated in the leading approximation of chiral perturbation theory, i.e., up to terms of $O(p^4)$ [8].

To probe the T-odd effect we introduce, in addition to f_{odd}, the ξ-asymmetrical physical observable, which is defined as follows:

$$A_\xi=\frac{N_+-N_-}{N_++N_-}, \tag{1}$$

where N_+ and N_- are the numbers of events with $\xi>0$ and $\xi<0$, respectively. One can see that, while the A_ξ nominator depends on $f_{odd}(\xi)$ only, the denominator is proportional to $f_{even}(\xi)$, which makes this variable sensitive to ξ-odd effects.

As we will show later, the "background" SM one-loop contribution to f_{odd} is severely suppressed with respect to f_{even} ($f_{odd}/f_{even}\sim 10^{-4}$). This allows us to state that the

*Email address: andre@mx.ihep.su

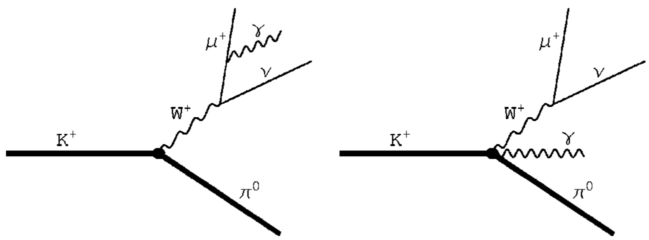

FIG. 1. The Feynman diagrams for the $K^+ \to \pi^0 l^+ \nu\gamma$ decay at the tree level of the SM.

proposed observables A_ξ and f_{odd}, sensitive to T-odd contributions, provide a good chance to search for CP-violating effects beyond the SM.

Another variable sensitive to CP violation is the transverse muon polarization P_T, which can be observed in the $K^+ \to \pi^0 \mu^+ \nu$ and $K^+ \to \mu^+ \nu\gamma$ decays [4,7,9]. As in the case of the ξ dependence of the $K^+ \to \pi^0 l^+ \nu_l \gamma$ rate, the presence of nonvanishing transverse polarization in the SM is caused by the electromagnetic final state interaction. Although the P_T value is sensitive to T-odd effects, its measurement in experiment seems to be cumbersome [10]. As for the A_ξ and f_{odd} variables, their experimental measurement is much easier, which is one of the main advantages of these variables in comparison with the transverse muon polarization. The low event rate of the processes where these values can be measured is considered to be the disadvantage of these variables. However, the anticipated statistics on the $K^+ \to \pi^0 \mu^+ \nu\gamma$ process in the OKA experiment will definitely allow one to use these observables to search for new CP-violating contributions.

In the next section we analyze the $K^+ \to \pi^0 l^+ \nu_l \gamma$ decay width dependence on the T-odd correlation at the tree level of the SM. In Sec. III we calculate SM contributions to the T-odd correlation induced by one-loop diagrams. The last section contains the discussion and conclusions.

II. *T*-ODD CORRELATION AT THE TREE LEVEL OF THE STANDARD MODEL

The Feynman diagrams contributing to the $K^+(p) \to \pi^0(p') l^+(p_l) \nu_l(p_\nu) \gamma(q)$ decay at the tree level of the SM are shown in Fig. 1. The tree-level amplitude for this process can be written as [8]

$$T = \frac{G_F}{\sqrt{2}} e V_{us}^* \epsilon^\mu(q)^* \bigg((V_{\mu\nu} - A_{\mu\nu}) \overline{u}(p_\nu) \gamma^\nu (1-\gamma_5) v(p_l) + \frac{F_\nu}{2p_l q} \overline{u}(p_\nu) \gamma^\nu (1-\gamma_5)(m_l - \hat{p}_l - \hat{q}) \gamma_\mu v(p_l) \bigg), \quad (2)$$

where

$$V_{\mu\nu} = i \int d^4x e^{iqx} \langle \pi^0(p') | T V_\mu^{em}(x) V_\nu^{4-i5}(0) | K^+(p) \rangle, \quad (3)$$

$$A_{\mu\nu} = i \int d^4x e^{iqx} \langle \pi^0(p') | T V_\mu^{em}(x) A_\nu^{4-i5}(0) | K^+(p) \rangle, \quad (4)$$

and F_ν is the matrix element of the K_{l3}^+ decay:

$$F_\nu = \langle \pi^0(p') | V_\nu^{4-i5}(0) | K^+(p) \rangle. \quad (5)$$

Here p', p_l, q, p_ν, and p are the pion, lepton, γ quantum, neutrino, and kaon four-momenta, respectively. In the leading approximation of chiral perturbation theory $A_{\mu\nu}=0$ and the expressions for $V_{\mu\nu}$ and F_μ can be written as

$$F_\mu = \frac{1}{\sqrt{2}} (p+p')_\mu,$$

$$V_{\mu\nu} = V_1 \left(g_{\mu\nu} - \frac{W_\mu q_\nu}{qW} \right) + V_2 \left(p'_\mu q_\nu - \frac{p'q}{qW} W_\mu q_\nu \right) + \frac{p_\mu}{pq} F_\nu,$$

$$W_\mu = (p_l + p_\nu)_\mu,$$

$$V_1 = \frac{1}{\sqrt{2}}, \quad V_2 = -\frac{1}{\sqrt{2} pq}.$$

So the matrix element of the decay can be rewritten in the following form:

$$T = \frac{G_F}{2} e V_{us}^* \epsilon^\mu(q)^* \cdot \overline{u}(p_\nu) \times (1+\gamma_5) \cdot \left[(\hat{p} + \hat{p}') \left(\frac{p_\mu}{(pq)} - \frac{(p_l)_\mu}{(p_l q)} \right) - (\hat{p} + \hat{p}') \frac{\hat{q}\gamma_\mu}{2(p_l q)} + \left(\gamma_\mu - \frac{\hat{q} p_\mu}{(pq)} \right) \right] u(p_l), \quad (6)$$

and the $K^+ \to \pi^0 l^+ \nu\gamma$ decay partial width can be calculated by integrating over the phase space.

In Figs. 2 and 3 we present the differential distribution of the decay partial width in the K-meson rest frame over the three-momenta of the final particles and the angle between the lepton and γ-quantum directions, calculated at the tree level of the SM. For the case of the electron channel (see Fig. 2) the bulk of the width value is collected in the region of small values of the lepton and γ-quantum momenta, maximal values of the pion momentum, and small angles between the lepton and γ-quantum momenta. In the case of the muon channel (see Fig. 3) the bulk of the width is collected in the region of intermediate values of lepton momentum, small values of the γ-quantum momentum, maximal values of the pion momentum, and small angles between the lepton and γ-quantum directions.

Imposing the kinematical cuts on the γ-quantum energy and lepton–γ-quantum scattering angle in the kaon rest

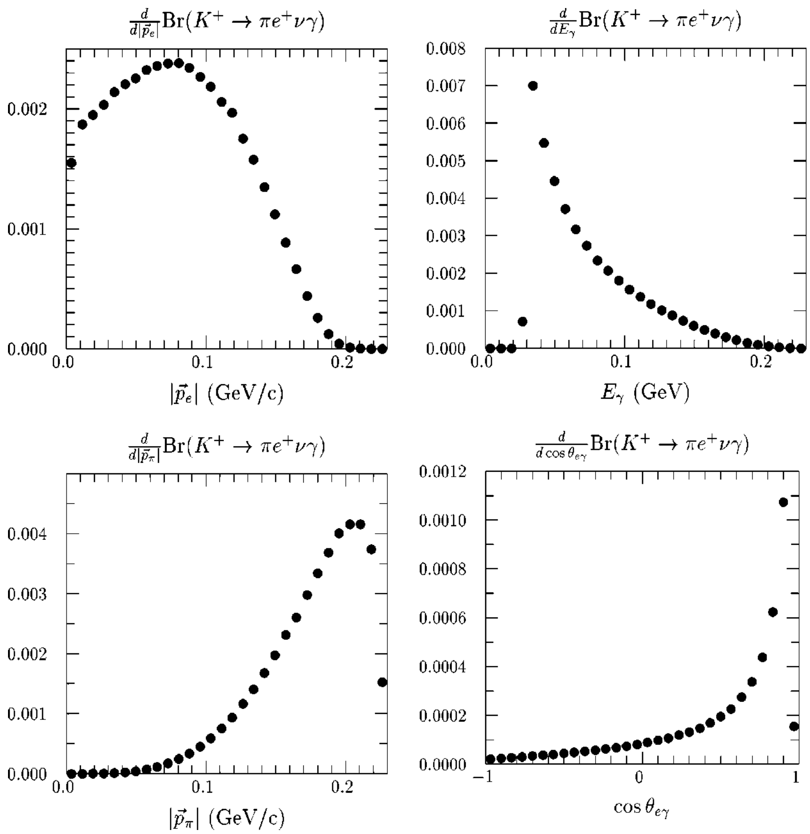

FIG. 2. Branching differential distribution over the pion, electron, and γ-quantum momenta and the angle between the electron and γ quantum in the K-meson rest frame.

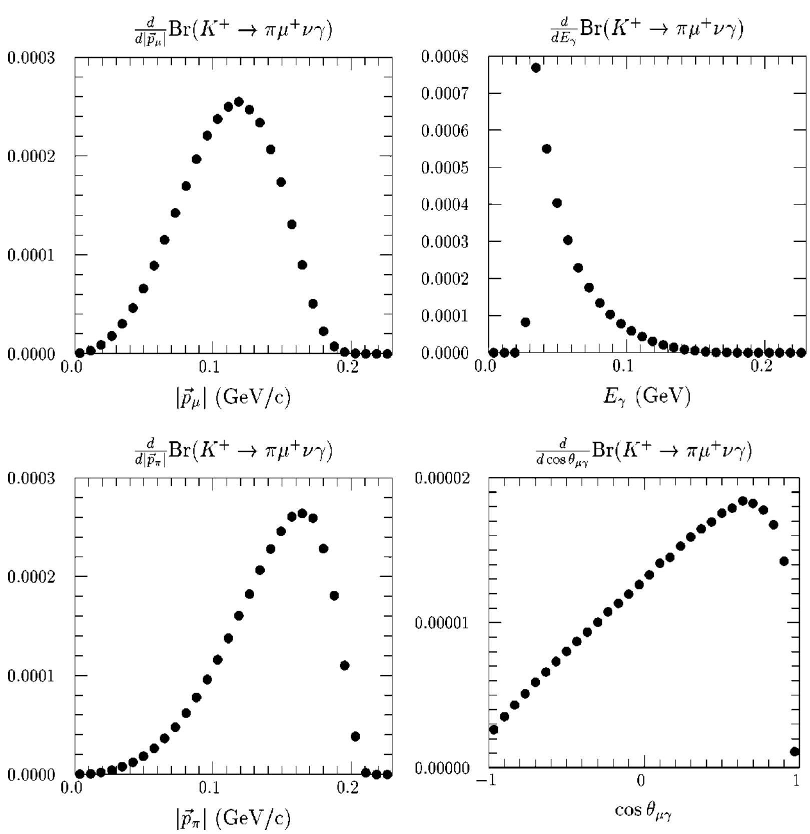

FIG. 3. Branching differential distribution over the pion, muon, and γ quantum momenta and the angle between the muon and γ quantum in the K-meson rest frame.

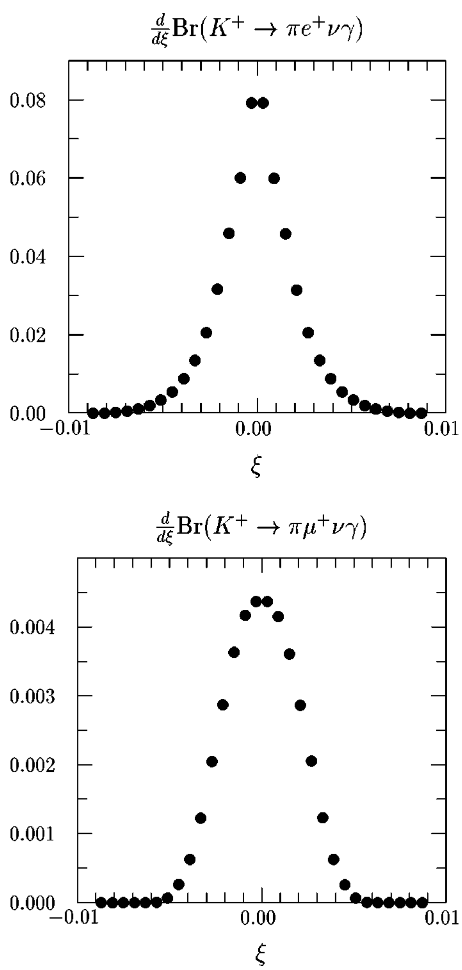

FIG. 4. ξ dependence of the $K^+ \to \pi^0 l^+ \nu\gamma$ branching at the tree level of the SM for the (a) electron and (b) muon channels.

frame $E_\gamma > 30$ MeV and $\theta_{\gamma l} > 20°$, which are typical for the current and planned kaon experiments, one gets the following branching values:

$$\mathrm{BR}(K^+ \to \pi e^+ \nu_e \gamma) = 3.18 \times 10^{-4},$$

$$\mathrm{BR}(K^+ \to \pi \mu^+ \nu_\mu \gamma) = 2.15 \times 10^{-5},$$

which are in good agreement with earlier calculations (see, for instance, [8]) and existing experimental results [11].

Looking for possible CP-odd contributions, we will investigate the decay width distribution over the variable $\xi = \vec{q} \cdot [\vec{p}_l \times \vec{p}_\pi]/M^3$, which changes sign under CP or T conjugation:

$$\rho(\xi) = \frac{d\Gamma}{d\xi}. \tag{7}$$

This distribution is an "indicator" for T-violation effects. The $\rho(\xi)$ function can be rewritten as

$$\rho = f_{even}(\xi) + f_{odd}(\xi),$$

where $f_{even}(\xi)$ and $f_{odd}(\xi)$ are the even and odd functions of ξ, respectively. The function $f_{odd}(\xi)$ can be represented as follows:

$$f_{odd} = g(\xi^2)\xi. \tag{8}$$

It is evident that after integration of the $\rho(\xi)$ function over whole region of ξ only the $f_{even}(\xi)$ function contributes to the total width. In Fig. 4 we present the $\rho(\xi)/\Gamma_{total}$ distributions for the $K^+ \to \pi^0 \mu^+ \nu_l \gamma$ and $K^+ \to \pi^0 e^+ \nu_l \gamma$ decays. Indeed, one can see from Fig. 4 that at the tree level of the SM, where there are no T-odd contributions, the distributions, as one would expect, are strictly symmetric with respect to the line $\xi = 0$, i.e., the numbers of events of $K^+ \to \pi^0 l^+ \nu_l \gamma$ decay with $\xi > 0$ and $\xi < 0$ are equal. This fact can be explained as follows: in the case of the tree approximation of the SM the matrix element squared is expressed via scalar products of final particle momenta only, and, consequently, there are no contributions linear over ξ. So the $\rho(\xi)$ function is essentially an even function of ξ.

Analyzing the $K^+ \to \pi^0 l^+ \nu_l \gamma$ data, it is useful to introduce, in addition to the $\rho(\xi)$ distribution, the integral asymmetry, which is defined as

$$A_\xi = \frac{N_+ - N_-}{N_+ + N_-}, \tag{9}$$

where N_+ and N_- are the numbers of decay events with $\xi > 0$ and $\xi < 0$. It is easy to see that the A_ξ nominator depends on $f_{odd}(\xi)$ only, which makes this variable highly sensitive to T-odd effects beyond the SM.

III. *T*-ODD CORRELATION IN THE STANDARD MODEL DUE TO THE FINAL STATE INTERACTION

A nonvanishing value of the A_ξ asymmetry as well as an odd contribution to $\rho(\xi)$ can arise in the SM due to the electromagnetic final state interaction at the level of one-loop diagrams. The most general expression for the $K^+ \to \pi^0 l^+ \nu_l \gamma$ decay amplitude taking account of the electromagnetic radiative corrections (implying gauge invariance) can be written as follows:

$$\begin{aligned} T_{one\ loop} = {} & \frac{G_F}{\sqrt{2}} e V_{us}^* \epsilon_\nu^* \overline{u}(p_\nu)(1+\gamma_5) \cdot \Bigg[C_1 \left(p^\nu - \frac{pq}{p_l q} p_l^\nu \right) \\ & + C_3 \left((p')^\nu - \frac{p'q}{p_l q} p_l^\nu \right) + C_5 \left(p^\nu - \frac{pq}{p_l q} p_l^\nu \right) \hat{p}' \\ & + C_7 \left((p')^\nu - \frac{p'q}{p_l q} p_l^\nu \right) \hat{p}' + C_9 [\hat{q} p^\nu - (pq)\gamma^\nu] \\ & + C_{10} [\hat{q} p_l^\nu - (p_l q)\gamma^\nu] + C_{11} [\hat{q}(p')^\nu - (p'q)\gamma^\nu] \\ & + C_{12} \hat{q}\gamma^\nu + C_{13} \hat{p}' [\hat{q} p^\nu - (pq)\gamma^\nu] + C_{14} \hat{p}' [\hat{q} p_l^\nu \\ & - (p_l q)\gamma^\nu] + C_{15} \hat{p}' [\hat{q}(p')^\nu - (p'q)\gamma^\nu] \\ & + C_{16} \hat{p}' \hat{q} \gamma^\nu \Bigg] v(p_l), \end{aligned} \tag{10}$$

where the C_i coefficients are the kinematical factors due to one-loop diagram contributions. The matrix element squared taking account of the one-loop contributions can be rewritten in the following form:

$$|T_{one\ loop}|^2=|T_{even}|^2+|T_{odd}|^2, \tag{11}$$

where

$$\begin{aligned}|T_{odd}|^2=&-2G_F^2e^2|V_{us}|^2m_K^4\xi\Bigg[\mathrm{Im}(C_1)m_l\left(2\frac{1}{p_lq}-4\frac{pq}{(p_lq)^2}\right)-\mathrm{Im}(C_3)m_l\left(2\frac{1}{p_lq}+4\frac{p'q}{(p_lq)^2}\right)+\mathrm{Im}(C_5)\\&\times\left(4+2m_l^2\frac{pq}{(p_lq)^2}+\frac{1}{p_lq}(2m_K^2-2m_\pi^2+4pp'-4pp_l-4pq-4p'p_l-4p'q)\right)+\mathrm{Im}(C_7)\left(2m_l^2\frac{p'q}{(p_lq)^2}+4\frac{m_\pi^2}{p_lq}\right)\\&+\mathrm{Im}(C_9)\left(8\frac{pp_l}{p_lq}-8\frac{m_K^2}{pq}\right)+\mathrm{Im}(C_{10})\left(8\frac{m_l^2}{p_lq}+8\frac{p_lq}{pq}-8\frac{pp_l}{pq}-8\right)+\mathrm{Im}(C_{11})\left(8\frac{p'q}{pq}+8\frac{p'p_l}{p_lq}-8\frac{pp'}{pq}\right)+\mathrm{Im}(C_{12})\\&\times\left(4\frac{m_l}{pq}-8\frac{m_l}{p_lq}\right)+\mathrm{Im}(C_{13})m_l\left(4\frac{m_K^2}{pq}-4\frac{pp_l}{p_lq}\right)+\mathrm{Im}(C_{14})m_l\left(4+4\frac{pp_l}{pq}-4\frac{m_l^2}{p_lq}-4\frac{p_lq}{pq}\right)+\mathrm{Im}(C_{15})m_l\\&\times\left(4\frac{pp'}{pq}-4\frac{p'q}{pq}-4\frac{p'p_l}{p_lq}\right)+\mathrm{Im}(C_{16})\left(-8+4\frac{m_K^2}{pq}-4\frac{m_\pi^2}{pq}+8\frac{pp'}{pq}-8\frac{pp_l}{pq}-8\frac{p'p_l}{pq}-8\frac{p'q}{pq}+4\frac{m_l^2}{p_lq}+8\frac{p_lq}{pq}\right)\Bigg].\end{aligned} \tag{12}$$

As one can see from Eqs. (11) and (12), the nonvanishing contribution to $f_{odd}(\xi)$ and A_ξ (linear over ξ) is determined by the one-loop electromagnetic corrections, which lead to the appearance of imaginary parts of the C_i form factors.

To calculate the form factor imaginary parts one can use the S-matrix unitarity [7]:

$$S^+S=1.$$

Using $S=1+iM$, one gets

$$M_{fi}-M_{if}^*=i\sum_n M_{nf}^*M_{ni}, \tag{13}$$

where the i,f,n indices correspond to the initial, final, and intermediate states of the particle system. Further, using the T invariance of the matrix element one has

$$\mathrm{Im}M_{fi}=\frac{1}{2}\sum_n M_{nf}^*M_{ni},$$

$$M_{fi}=(2\pi)^4\delta(P_f-P_i)T_{fi}.$$

One-loop diagrams that describe the electromagnetic corrections to the $K^+\to\pi l^+\nu_l\gamma$ process and lead to imaginary parts of the form factors in Eq. (10), thus contributing to $f_{odd}(\xi)$, are shown in Fig. 5. Using Eq. (2) one can write down the imaginary parts of these diagrams, that give the nonvanishing contribution to $f_{odd}(\xi)$. It is useful to split the whole set of one-loop diagrams into two groups. The first group contains the diagrams shown in Figs. 5a, 5c, and 5e. The imaginary part of these diagrams can be written as follows:

$$\begin{aligned}\mathrm{Im}T_1=&\frac{\alpha}{2\pi}\frac{G_F}{\sqrt{2}}eV_{us}^*\overline{u}(p_\nu)(1+\gamma_5)\int\frac{d^3k_\gamma}{2\omega_\gamma}\frac{d^3k_l}{2\omega_l}\\&\times\delta(k_\gamma+k_l-q-p_l)\cdot|\hat{R}_\mu(\hat{k}_l-m_l)\gamma^\mu\\&\times\frac{\hat{q}+\hat{p}_l-m_l}{(q+p_l)^2-m_l^2}\gamma^\delta\varepsilon_\delta^*v(p_l).\end{aligned} \tag{14}$$

The second group includes the diagrams shown in Figs. 5b, 5d, and 5f. The corresponding imaginary part is

$$\begin{aligned}\mathrm{Im}T_2=&\frac{\alpha}{2\pi}\frac{G_F}{\sqrt{2}}eV_{us}^*\overline{u}(p_\nu)(1+\gamma_5)\int\frac{d^3k_\gamma}{2\omega_\gamma}\frac{d^3k_l}{2\omega_l}\\&\times\delta(k_\gamma+k_l-q-p_l)\cdot\hat{R}_\mu(\hat{k}_l-m_l)\\&\times\gamma^\delta\varepsilon_\delta^*\frac{\hat{k}_\mu-\hat{q}-m_l}{(k_\mu-q)^2-m_l^2}\gamma^\mu v(p_l),\end{aligned} \tag{15}$$

where

$$\hat{R}_\mu=(V_{\mu\nu}-A_{\mu\nu})\gamma^\nu-\frac{F_\nu}{2p_lq}\gamma^\nu(\hat{p}_l+\hat{q}-m_l)\gamma_\mu. \tag{16}$$

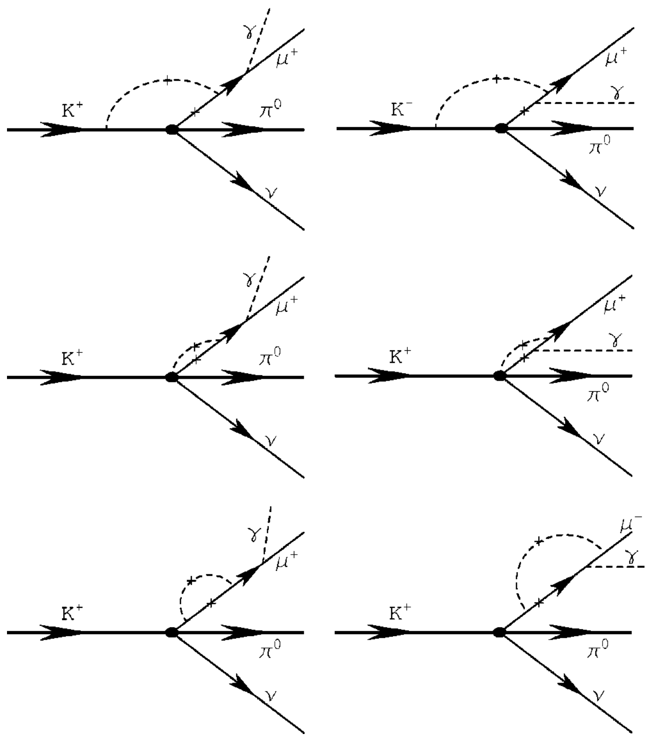

FIG. 5. The Feynman diagrams contributing to the imaginary parts of the form factors (10) at the one-loop level of the SM.

The details of the calculation of the integrals entering Eqs. (14),(15) and their dependence on kinematical parameters are given in Appendix A. The expressions for the imaginary parts of the C_i form factors are given in Appendix B.

IV. RESULTS AND DISCUSSION

Before discussing the numerical results, let us note that when considering one-loop diagrams we neglected their contributions to the even part of the ξ distribution, as these contributions are considerably smaller than the nonzero contribution to f_{even} from the tree approximation of the SM. However, in the case of f_{odd} the tree SM contribution is equal to zero; thus the contributions to f_{odd} coming from one-loop diagrams become essential. Analyzing the $K^+ \to \pi^0 l^+ \nu_l \gamma$ width dependence on the kinematical variable ξ, we separately consider the two decay channels $K^+ \to \pi^0 e^+ \nu_e \gamma$ and $K^+ \to \pi^0 \mu^+ \nu_\mu \gamma$, since the functional ξ dependence of the width in these two cases is essentially different.

$K^+ \to \pi^0 e^+ \nu_e \gamma$. In Fig. 6a we show the ξ-odd contribution to the differential width distribution that is induced by the imaginary parts of the one-loop diagrams shown in Fig. 5. In the kinematical region of the ξ parameter the value of the width distribution varies in the interval of $(-2.0\text{–}2.0) \times 10^{-6}$, and the sign of f_{odd} is opposite to the sign of ξ. As the total ξ distribution is the sum of the even and odd parts, this leads to the fact that in an experiment one will observe the surplus of the events with negative ξ values. The asymmetry value for this channel is

$$A_\xi(K^+ \to \pi e^+ \nu_e \gamma) = -0.59 \times 10^{-4}.$$

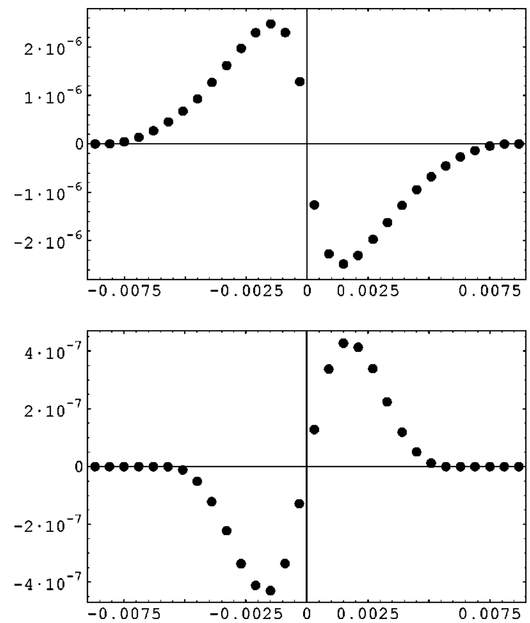

FIG. 6. ξ-odd contributions f_{odd} to the branching differential distribution for the (a) electron and (b) muon decay channels.

$K^+ \to \pi^0 \mu^+ \nu_\mu \gamma$. In Fig. 6b we present the ξ-odd contribution to the differential width distribution for the muon decay channel. The characteristic variation interval for this distribution is $(-4.0\text{–}4.0) \times 10^{-7}$, but the sign of f_{odd} coincides with the sign of ξ. This results in a surplus of events with positive ξ values. The asymmetry value for this channel is

$$A_\xi(K^+ \to \pi \mu^+ \nu_\mu \gamma) = 1.14 \times 10^{-4}.$$

This difference between the f_{odd} behavior in the cases of the electron and muon channels can be explained as follows: for the muon decay channel the contributions from imaginary parts of the C_1, C_{12}, C_{13}, and C_{14} form factors become essential, while in the case of the electron channel their contributions are negligible (these contributions are proportional to the mass of the lepton).

It should be noted that the difference in the f_{odd} behavior for the electron and muon channels could be used to disentangle the SM radiative and new physics contributions: in extended models, where the CP violation can arise at tree level, the sign of the ξ dependence is insensitive to the lepton flavor, as occurs, for instance, in the Weinberg model [1].

We would like to underline that for both decay channels the f_{odd} value is four orders of magnitude smaller than the tree contribution of the SM. This allows us to state that ξ-odd effects are severely suppressed in the SM. Thus, the "background" SM contribution to the odd part of the ξ dependence leaves a "window" to discover new CP-violating effects in these decays up to the level of 10^{-4}.

Analyzing the situation with the integral asymmetry A_ξ one sees that for reliable observation of ξ-odd effects from the asymmetry only one should have a data sample for these decays at least at the level of 10^8 events. In this respect analysis of the differential ξ distribution seems to be very important.

ACKNOWLEDGMENTS

The authors would like to thank L. B. Okun for critical remarks and interest in this calculations and to acknowledge useful discussions with and valuable remarks by V. A. Rubakov, A. K. Likhoded, and V. F. Obraztsov. This work was supported, in part, by the RFBR, Grant Nos. 99-02-16558 and 00-15-96645, and the RF Ministry of Education, grant 00-3.3-62.

APPENDIX A

In calculating the integrals that contribute to Eqs. (14) and (15), we use the following notation:

$$P=p_l+q,$$

$$d\rho=\frac{d^3k_\gamma}{2\omega_\gamma}\frac{d^3k_l}{2\omega_l}\delta(k_\gamma+k_l-P).$$

We present below either the explicit expressions for the integrals, or the set of equations that, being solved, give the parameters entering the integrals:

$$J_{11}=\int d\rho=\frac{\pi}{2}\frac{P^2-m_l^2}{P^2},$$

$$J_{12}=\int d\rho\frac{1}{(pk_\gamma)}=\frac{\pi}{2I}\ln\left(\frac{(Pp)+I}{(Pp)-I}\right),$$

where

$$I^2=(Pp)^2-m_K^2P^2,$$

$$\int d\rho\frac{k_\gamma^\alpha}{(pk_\gamma)}=a_{11}p^\alpha+b_{11}P^\alpha.$$

The a_{11} and b_{11} parameters are defined as follows:

$$a_{11}=-\frac{1}{(Pp)^2-m_K^2P^2}\left(P^2J_{11}-\frac{J_{12}}{2}(Pp)(P^2-m_l^2)\right),$$

$$b_{11}=\frac{1}{(Pp)^2-m_K^2P^2}\left((Pp)J_{11}-\frac{J_{12}}{2}m_K^2(P^2-m_l^2)\right).$$

$$\int d\rho k_\gamma^\alpha=a_{12}P^\alpha,$$

where

$$a_{12}=\frac{(P^2-m_l^2)}{2P^2}J_{11},$$

$$J_1=\int d\rho\frac{1}{(pk_\gamma)((p_l-k_\gamma)^2-m_l^2)}$$
$$=-\frac{\pi}{2I_1(P^2-m_l^2)}\ln\left(\frac{(pp_l)+I_1}{(pp_l)-I_1}\right),$$

$$J_2=\int d\rho\frac{1}{(p_l-k_\gamma)^2-m_l^2}$$
$$=-\frac{\pi}{4I_2}\ln\left(\frac{(Pp_l)+I_2}{(Pp_l)-I_2}\right),$$

where

$$I_1^2=(pp_l)^2-m_l^2m_K^2,$$
$$I_2^2=(Pp_l)^2-m_l^2P^2.$$

$$\int d\rho\frac{k_\gamma^\alpha}{(p_l-k_\gamma)^2-m_l^2}=a_1P^\alpha+b_1p_l^\alpha,$$

$$a_1=-\frac{m_l^2(P^2-m_l^2)J_2+(Pp_l)J_{11}}{2((Pp_l)^2-m_l^2P^2)},$$

$$b_1=\frac{(Pp_l)(P^2-m_l^2)J_2+P^2J_{11}}{2[(Pp_l)^2-m_l^2P^2]}.$$

The integrals below are expressed in terms of the parameters, which can be obtained by solving the corresponding sets of equations:

$$\int d\rho\frac{k_\gamma^\alpha}{(pk_\gamma)[(p_l-k_\gamma)^2-m_l^2]}=a_2P^\alpha+b_2p^\alpha+c_2p_l^\alpha,$$

$$a_2(Pp)+b_2m_K^2+c_2(pp_l)=J_2,$$

$$a_2(Pp_l)+b_2(pp_l)+c_2m_l^2=-\frac{1}{2}J_{12},$$

$$a_2P^2+b_2(Pp)+c_2(Pp_l)=(p_lq)J_1.$$

$$\int d\rho\frac{k_\gamma^\alpha k_\gamma^\beta}{(pk_\gamma)[(p_l-k_\gamma)^2-m_l^2]}=a_3g^{\alpha\beta}+b_3(P^\alpha p^\beta+P^\beta p^\alpha)$$
$$+c_3(P^\alpha p_l^\beta+P^\beta p_l^\alpha)$$
$$+d_3(p^\alpha p_l^\beta+p^\beta p_l^\alpha)$$
$$+e_3p_l^\alpha p_l^\beta+f_3P^\alpha P^\beta$$
$$+g_3p^\alpha p^\beta,$$

$$4a_3+2b_3(Pp)+2c_3(Pp_l)+2d_3(pp_l)$$
$$+g_3m_K^2+e_3m_l^2+f_3P^2=0,$$

$$c_3(pp_l)+b_3m_K^2+f_3(Pp)-a_1=0,$$

$$c_3(Pp)+d_3m_K^2+e_3(pp_l)-b_1=0,$$

$$a_3+b_3(Pp)+d_3(pp_l)+g_3m_K^2=0,$$

$$b_3(pp_l)+c_3m_l^2+f_3(Pp_l)=-\frac{1}{2}b_{11},$$

$$b_3(Pp_l)+d_3m_l^2+g_3(pp_l)=-\frac{1}{2}a_{11},$$

$$a_3P^2+2b_3P^2(Pp)+2c_3P^2(Pp_l)+2d_3(Pp_l)(Pp)+e_3(Pp_l)^2+f_3(P^2)^2+g_3(Pp)^2=(p_lq)^2J_1.$$

$$\int d\rho\frac{k_\gamma^\alpha k_\gamma^\beta}{(p_l-k_\gamma)^2-m_l^2}=a_4g_{\alpha\beta}+b_4(P^\alpha p_l^\beta+P^\beta p_l^\alpha)+c_4P^\alpha P^\beta+d_4p_l^\alpha p_l^\beta,$$

$$a_4+d_4m_l^2+b_4(Pp_l)=0,$$

$$b_4m_l^2+c_4(Pp_l)=-\frac{1}{2}a_{12},$$

$$4a_4+2b_4(Pp_l)+c_4P^2+d_4m_l^2=0,$$

$$a_4P^2+2b_4P^2(Pp_l)+c_4(P^2)^2+d_4(Pp_l)^2=\frac{(P^2-m_l^2)^2}{4}J_2$$

APPENDIX B

Here we present the explicit expressions for imaginary parts of the C_i form factors via the parameters calculated in Appendix A.

$$C_1=\frac{\alpha}{\sqrt{2}\pi}m_l[4a_3+b_3m_K^2+d_3m_K^2-2a_2m_l^2+2b_3m_l^2-2c_2m_l^2+6c_3m_l^2+2d_3m_l^2+3e_3m_l^2+3f_3m_l^2-b_3m_\pi^2-d_3m_\pi^2-2b_3(p'p_l-2d_3(p'p_l)-2b_3(p'q)-2d_3(p'q)-4a_2(p_lq)+4b_3(p_lq)-2c_2(p_lq)+8c_3(p_lq)+2d_3(p_lq)+2e_3(p_lq)+6f_3(p_lq)+2b_3(pp')+2d_3(pp'),$$

$$C_5=-\frac{\alpha}{\sqrt{2}\pi}[4a_3-4a_2m_l^2+3b_3m_l^2-4c_2m_l^2+4c_3m_l^2+3d_3m_l^2+2e_3m_l^2+2f_3m_l^2-4a_2(p_lq)+4b_3(p_lq)+4c_3(p_lq)+4f_3(p_lq)],$$

$$C_9=-\frac{\alpha}{\sqrt{2}\pi}[2a_3+b_3m_K^2-a_2m_l^2+b_3m_l^2-c_2m_l^2+2c_3m_l^2+d_3m_l^2+2f_3m_l^2-b_3m_\pi^2-2b_3(p'p_l)-2b_3(p'q)-2a_2(p_lq)+2b_3(p_lq)+2c_3(p_lq)+4f_3(p_lq)+2b_3(pp')],$$

$$C_{10}=\frac{\alpha}{\sqrt{2}\pi}\frac{1}{(p_lq)}[-a_1m_l^2-b_1m_l^2+2b_4m_l^2+c_4m_l^2+d_4m_l^2+2a_3(p_lq)+a_2m_K^2(p_lq)-c_3m_K^2(p_lq)-f_3m_K^2(p_lq)-e_3m_l^2(p_lq)+f_3m_l^2(p_lq)-a_2m_\pi^2(p_lq)+c_3m_\pi^2(p_lq)+f_3m_\pi^2(p_lq)-2a_2(p'p_l)(p_lq)+2c_3(p'p_l)(p_lq)+2f_3(p'p_l)(p_lq)-2a_2(p'q)(p_lq)+2c_3(p'q)(p_lq)+2f_3(p'q)(p_lq)+2f_3(p_lq)^2+2a_2(p_lq)(pp')-2c_3(p_lq)\times(pp')-2f_3(p_lq)(pp')-2a_2(p_lq)(pp_l)+2b_3(p_lq)(pp_l)+2c_3(p_lq)(pp_l)+2f_3(p_lq)(pp_l)-2a_2(p_lq)(pq)+2b_3(p_lq)(pq)+2c_3(p_lq)(pq)+2f_3(p_lq)(pq)],$$

$$
\begin{aligned}
C_{12}=&-\frac{\alpha}{4\sqrt{2}\pi}\frac{m_l}{(p_lq)^2}[-2a_{12}m_l^2-2J_{11}m_l^2-2a_{12}(p_lq)-4a_4(p_lq)+2J_{11}(p_lq)-a_{11}m_K^2(p_lq)+b_{11}m_K^2(p_lq)\\
&+8a_1m_l^2(p_lq)+8b_1m_l^2(p_lq)-4b_4m_l^2(p_lq)-2c_4m_l^2(p_lq)-2d_4m_l^2(p_lq)-4J_2m_l^2(p_lq)-b_{11}m_\pi^2(p_lq)\\
&-2b_{11}(p'p_l)(p_lq)-2b_{11}(p'q)(p_lq)+8a_1(p_lq)^2+4a_3(p_lq)^2+4b_1(p_lq)^2-4b_4(p_lq)^2-4c_4(p_lq)^2\\
&-4J_2(p_lq)^2+2a_2m_K^2(p_lq)^2-2b_2m_K^2(p_lq)^2+2c_2m_K^2(p_lq)^2+2g_3m_K^2(p_lq)^2+8c_3m_l^2(p_lq)^2+6e_3m_l^2(p_lq)^2\\
&+2f_3m_l^2(p_lq)^2-2a_2m_\pi^2(p_lq)^2-2c_2m_\pi^2(p_lq)^2-4a_2(p'p_l)(p_lq)^2-4c_2(p'p_l)(p_lq)^2-4a_2(p'q)(p_lq)^2\\
&-4c_2(p'q)(p_lq)^2+12c_3(p_lq)^3+4e_3(p_lq)^3+4f_3(p_lq)^3+2b_{11}(p_lq)(pp')+4a_2(p_lq)^2(pp')+4c_2(p_lq)^2(pp')\\
&-2a_{11}(p_lq)(pp_l)-4b_{11}(p_lq)(pp_l)+2J_{12}(p_lq)(pp_l)-8a_2(p_lq)^2(pp_l)-4b_2(p_lq)^2(pp_l)+4b_3(p_lq)^2(pp_l)\\
&-8c_2(p_lq)^2(pp_l)+8d_3(p_lq)^2(pp_l)+4J_1(p_lq)^2(pp_l)-2a_{11}(p_lq)(pq)-4b_{11}(p_lq)(pq)+2J_{12}(p_lq)(pq)\\
&-4a_2(p_lq)^2(pq)+4b_3(p_lq)^2(pq)-4c_2(p_lq)^2(pq)+4d_3(p_lq)^2(pq)],
\end{aligned}
$$

$$C_{13}=-\frac{\alpha}{\sqrt{2}\pi}m_l(2a_2-b_3+2c_2-2d_3),$$

$$C_{14}=\frac{\alpha}{\sqrt{2}\pi}\frac{m_l}{(p_lq)}[2a_1+2b_1-4b_4-2c_4-2d_4+a_2(p_lq)+3c_3(p_lq)+2e_3(p_lq)+f_3(p_lq)],$$

$$
\begin{aligned}
C_{16}=&\frac{\alpha}{4\sqrt{2}\pi}\frac{1}{(p_lq)^2}[-4a_{12}m_l^2-4J_{11}m_l^2-4a_{12}(p_lq)-8a_4(p_lq)+4J_{11}(p_lq)-2a_{11}m_K^2(p_lq)+16a_1m_l^2(p_lq)\\
&+16b_1m_l^2(p_lq)+b_{11}m_l^2(p_lq)-8b_4m_l^2(p_lq)-4c_4m_l^2(p_lq)-4d_4m_l^2(p_lq)-8J_2m_l^2(p_lq)+16a_1(p_lq)^2\\
&+4a_3(p_lq)^2+8b_1(p_lq)^2-8b_4(p_lq)^2-8c_4(p_lq)^2-2J_{12}(p_lq)^2-8J_2(p_lq)^2-4b_2m_K^2(p_lq)^2+4g_3m_K^2(p_lq)^2\\
&-2a_2m_l^2(p_lq)^2-2c_2m_l^2(p_lq)^2+4c_3m_l^2(p_lq)^2+4e_3m_l^2(p_lq)^2-4a_2(p_lq)^3+4c_3(p_lq)^3-2a_{11}(p_lq)(pp_l)\\
&-4b_{11}(p_lq)(pp_l)+4J_{12}(p_lq)(pp_l)-8a_2(p_lq)^2(pp_l)-8b_2(p_lq)^2(pp_l)+4b_3(p_lq)^2(pp_l)-8c_2(p_lq)^2(pp_l)\\
&+8d_3(p_lq)^2(pp_l)+8J_1(p_lq)^2(pp_l)-2a_{11}(p_lq)(pq)-4b_{11}(p_lq)(pq)+4J_{12}(p_lq)(pq)+4b_3(p_lq)^2(pq)],
\end{aligned}
$$

$$C_3=C_7=C_{11}=C_{15}=0.$$

[1] S. Weinberg, Phys. Rev. Lett. **37**, 651 (1976).
[2] R.J. Tesarek, hep-ex/9903069.
[3] A. Likhoded, V. Braguta, and A. Chalov (unpublished); see also, V.F. Obraztosv *et al.*, hep-ex/0011033.
[4] V. Braguta, A. Likhoded, and A. Chalov, hep-ph/0105111.
[5] V.F. Obraztsov, Nucl. Phys. B (Proc. Suppl.) **99**, 257 (2001).
[6] J.F. Donoghue and B. Holstein, Phys. Lett. **113B**, 382 (1982); L. Wolfenstein, Phys. Rev. D **29**, 2130 (1984); G. Barenboim *et al.*, Phys. Rev. D **55**, 4213 (1997); M. Kobayashi, T.-T. Lin, and Y. Okada, Prog. Theor. Phys. **95**, 361 (1996); S.S. Gershtein *et al.*, Z. Phys. C **24**, 305 (1984); R. Garisto and G. Kane, Phys. Rev. D **44**, 2038 (1991); G. Belanger and C.Q. Cheng, *ibid.* **44**, 2789 (1991).
[7] L.B. Okun and I.B. Khriplovich, Sov. J. Nucl. Phys. **6**, 821 (1967).
[8] J. Bijnens, G. Ecker, and J. Gasser, Nucl. Phys. **B396**, 81 (1993).
[9] A.R. Zhitnitskii, Sov. J. Nucl. Phys. **31**, 529 (1980); see also C.Q. Geng and J.N. Ng, Phys. Rev. D **42**, 1509 (1990); C.H. Chen, C.Q. Geng, and C.C. Lih, *ibid.* **56**, 6856 (1997); G. Hiller and G. Isidori, Phys. Lett. B **459**, 295 (1999).
[10] See, for instance, Yu.G. Kudenko, hep-ex/0103007.
[11] Particle Data Group, D. Groom *et al.*, Eur. Phys. J. C **15**, 1 (2000), p. 501.